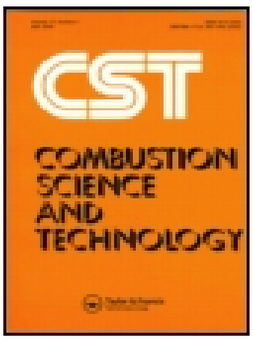

COMBUSTION SCIENCE AND TECHNOLOGY

ISSN: 0010-2202 (Print) 1563-521X (Online) Journal homepage: https://www.tandfonline.com/loi/gcst20

Turbulent Premixed Hydrogen/Air Flames at High Reynolds Numbers

M. S. WU , S. KWON , J. F. DRISCOLL & G. M. FAETH

To cite this article: M. S. WU , S. KWON , J. F. DRISCOLL & G. M. FAETH (1990) Turbulent Premixed Hydrogen/Air Flames at High Reynolds Numbers, COMBUSTION SCIENCE AND TECHNOLOGY, 73:1-3, 327-350, DOI: 10.1080/00102209008951655

To link to this article: https://doi.org/10.1080/00102209008951655

Combust. Sci. and Tech., 1990, Vol. 73, pp. 327–350
Photocopying permitted by license only

Turbulent Premixed Hydrogen/Air Flames at High Reynolds Numbers

M.-S. WU, S. KWON, J. F. DRISCOLL and G. M. FAETH *Department of Aerospace Engineering, The University of Michigan, Ann Arbor, Michigan 48109-2140*

(*Received July 24, 1989; in final form April 23, 1990*)

Abstract—Measurements of mean and fluctuating reaction progress variable and streamwise velocities are reported for turbulent premixed hydrogen/air flames burning at relatively high Reynolds numbers (up to 1800, based on streamwise r.m.s. velocity fluctuations and integral length scales). A round-jet geometry was used with the flame surrounded by a hot combustion-gas environment at atmospheric pressure. Mixing-limited combustion was achieved: values of r.m.s. velocity fluctuations, normalized by the laminar burning velocity ($\tilde{u}'/S_L$), exceeded 15 in some instances. Test conditions included fuel-equivalence ratios of 0.3–3.6 and burner exit Reynolds numbers (based on exit diameter) of 7000–40 000 with fully-developed turbulent pipe flow at the burner exit. It was found that effects of diffusive-thermal (preferential-diffusion) phenomena were important, for both stable (fuel-equivalence ratios greater than 1.8) and unstable conditions, even at the present high Reynolds numbers; for example, flame surfaces were more spiked and effective turbulent burning velocities for unstable conditions were twice as large as burning velocities for stable conditions having comparable normalized turbulence levels ($\tilde{u}'/S_L$). The measurements were used to evaluate contemporary turbulence models of premixed flames that are based on the laminar flamelet concept and which allow for effects of flame stretch: predictions yielded only fair agreement with measurements, partly due to the fact that the models ignore effects of finite laminar flame speeds and diffusive-thermal (preferential diffusion) phenomena that are found to be particularly important for hydrogen/air flames.

NOMENCLATURE

a	acceleration of gravity
c	reaction progress variable
C_i	constants in turbulence model
d	burner exit diameter
g	constant in reaction rate expression
G	generic property
I_o	flamelet quench integral
k	turbulence kinetic energy
l	integral length scale
l_K	Kolmogorov length scale
L_c	flame length based on $\tilde{c}_c = 0.5$
r	radial distance
Re	burner exit Reynolds number
S_L	laminar burning velocity
$S_{T,\text{eff}}$	effective turbulent burning velocity
S_G	source term in governing equations
u	streamwise velocity
x	streamwise distance
v	radial velocity

Address Correspondence to: G. M. Faeth, 218 Aerospace Engineering Building, The University of Michigan, Ann Arbor, MI 48109-2140.

Greek Letters

α	thermal diffusivity
δ_L	laminar flame thickness
ε	rate of dissipation of turbulence kinetic energy
ε_q	rate of dissipation at quenching condition
μ_t	turbulent viscosity
ν	kinematic viscosity
ρ	density
σ	standard-deviation of log-normal distribution
σ_G	turbulent Prandtl/Schmidt number
$\lvert\sigma_y\rvert$	crossing angle factor
τ	heat release parameter
ϕ	fuel-equivalence ratio

Subscripts

avg	average value
c	centerline value
o	burner exit condition

Superscripts

$(\tilde{\ })$	Favre-averaged mean property
$(\bar{\ })$, $(\bar{\ })'$	time-averaged mean and r.m.s. fluctuating property

INTRODUCTION

Turbulent premixed flames are an important fundamental combustion problem with numerous practical applications; therefore, they have received significant attention in the past. Nevertheless, Libby *et al.* (1986) point out that additional measurements are needed to develop and evaluate theories of turbulent premixed flames. The main problems are that existing measurements either involve complex flow configurations that are difficult to compute accurately, or moderate Reynolds numbers where the degree of development of the turbulence and the intrusion of buoyancy may not be representative of practical flames. The objective of the present investigation was to help address these limitations by measuring the structure of turbulent hydrogen/air jet flames at high Reynolds numbers. Hydrogen/air flames were studied since they are of interest for several advanced propulsion and metal cutting applications and they place unusual stress on concepts of modeling turbulent flames, *e.g.*, they have unusually high laminar flame speeds and are subject to diffusive-thermal instabilities due to preferential diffusion of hydrogen. Thus, to help quantify the potential significance of these phenomena, the measurements were also used to evaluate predictions of contemporary turbulence models of the process.

Hydrodynamic and diffusive-thermal instabilities are the two main mechanisms of instability of premixed flames when effects of buoyancy are small (Williams, 1989). However, while hydrodynamic instability has been observed in special circumstances (Groff, 1982), it is generally agreed that most observations of laminar flame instability can be traced to diffusive-thermal effects (Markstein, 1951). The preferential-diffusion mechanism that is associated with diffusive-thermal instability is particularly relevant to the behavior of hydrogen/air flames due to the unusually high mass diffusivity of

hydrogen in comparison to other stable species in flames (Williams, 1985). Preferential diffusion involves the interaction between transverse diffusion of a faster-diffusing reactant and the variation of the laminar flame speed with the unreacted gas composition (Manton *et al.*, 1952). Since the flame serves as a sink for reactants, the faster-diffusing species accumulates near upstream-pointing bulges in the flame surface and is depleted from downstream-pointing bulges. For fuel-equivalence ratios at which the laminar flame speed increases with increasing concentration of the fast-diffusing constituent, the bulges grow and the flame is unstable. Hydrogen is the faster-diffusing constituent for hydrogen/air flames; therefore, these flames are unstable for fuel-equivalence ratios less than 1.8, at which the maximum laminar flame speed is reached (Andrews and Bradley, 1973; Lewis and von Elbe, 1961). Indeed, Andrews and Bradley (1973) and Halstead *et al.* (1974) have observed that certain fuel-lean hydrogen/air flames are unstable. The hydrogen/air system is somewhat unique in this respect: most other fuel/air systems have maximum laminar flame speeds near a fuel-equivalence ratio of unity; and most other fuels (except for methane) are heavier than air and are unstable for fuel-rich conditions.

Although diffusive-thermal phenomena have been primarily studied to explain instabilities of premixed flames propagating in laminar environments, they can still influence flames in turbulent environments where the flame surface is distorted by turbulent fluctuations. Clavin and coworkers have studied these effects using asymptotic analysis and measurements in turbulent flows having large scale and low intensity (Boyer *et al.*, 1980; Clavin, 1985; Clavin and Williams, 1979, 1982; Searby and Clavin, 1986). Turbulent deflections of the flame surface were found to be chaotically enhanced for unstable conditions; in contrast, the flame acted like a high-pass filter, damping low-frequency turbulent deflections of its surface for stable conditions. The conditions of these studies involved only weak turbulence, however, and are rather far removed from highly-turbulent premixed flames; therefore, the importance of diffusive-thermal phenomena for practical turbulent flames, as shown in the following, has not been established previously.

Rigorous asymptotic analysis or exact numerical simulations have not progressed to the point where they can treat practical turbulent premixed flames; therefore, turbulence models have received significant attention (see Bray (1980), Cant and Bray (1988), Jones and Whitelaw (1982), Libby *et al.* (1986) and references cited therein). These methods are generally limited to high Reynolds number turbulent flows at the laminar-flamelet limit where the reaction zone is thin compared to the smallest length scales of the turbulence. Initial work involved either eddy-breakup ideas or thin laminar flamelets at the mixing-controlled limit where effects of the details of laminar flamelet structure are small (Bray, 1980). Recent methods, however, consider effects of quenching due to flame stretch—an important turbulence/chemistry interaction at high Reynolds numbers (Cant and Bray, 1988). Nevertheless, existing methods tacitly ignore effects of finite laminar flame speeds and diffusive-thermal phenomena that may be important in some instances. Furthermore, these methods involve many other approximations and empiricisms that have not yet been evaluated by comparison with measurements.

In summary, it is important to assess whether diffusive-thermal effects, which are known to be important at low Reynolds numbers, are also important at high Reynolds numbers. Do they enhance turbulent burning velocities for unstable conditions, decrease turbulent burning velocities at stable conditions, and are these effects significant enough so that they should be considered in models of turbulent premixed flames? Thus, the main objectives of the present investigation were to measure the structure of premixed hydrogen/air jet flames (which are likely to exhibit diffusive-thermal (preferential diffusion) phenomena) at high Reynolds numbers; and to use

these results to evaluate the predictions of contemporary turbulence models along the lines of Bray (1980) and Cant and Bray (1988). Test conditions were as follows: $0.3 \leqslant \phi \leqslant 3.57$, which involves both unstable and stable regimes for preferential diffusion instability; $7000 \leqslant Re \leqslant 40\,000$, which insures reasonably well-developed turbulence over the test range; $0.4 \leqslant \bar{u}'_{o,avg}/S_L \leqslant 15.5$, to vary the relative importance of laminar and turbulent flame propagation effects; and $4 \leqslant \bar{u}_{o,avg}/S_L \leqslant 155$, so that the boundary-layer approximations could be used to analyze the flow, since mean flame angles with respect to the streamwise direction were relatively small. Measurements included flash-Schlieren photography for flow visualization, Rayleigh scattering for the extent of reaction, and laser velocimetry for streamwise velocities. Some limited observations of premixed hydrogen/air flames were also undertaken in a fan-stirred bomb in order to gain insight concerning diffusive-thermal behavior.

The paper begins with descriptions of experimental and theoretical methods. Results of flow visualization in the fan-stirred bomb and the jet flames are then discussed. The paper concludes with consideration of measurements of the extent of reaction and velocities, and their comparison with predictions.

EXPERIMENTAL METHODS

Apparatus

Jet burner Figure 1 is a sketch of the jet burner. A coaxial design was used, consisting of an inner round-jet burner having a diameter of 11 mm and a tube length-to-diameter ratio of 50, to yield nearly fully-developed turbulent pipe flow at the burner exit, and an outer burner having a diameter of 58 mm with the outer flame stabilized much like a flat-flame burner above a bed of beads and screens. The burners operated at atmospheric pressure with combustion products removed by a hood whose inlet was 1 m above the burner exit. Instruments were mounted rigidly; therefore, the burner was traversed in the radial (positioning accuracy of 10 μm) and vertical (positioning accuracy of 1000 μm) directions to measure flame structure.

All measurements were limited to the jet flame of the inner burner, while the outer burner flame only served to provide a hot environment to stabilize and reduce rates of entrainment of the jet flame. Since the velocities and mixture ratios of the outer and inner burners were not the same (as discussed later), there was a mixing layer between the two flows as sketched in Figure 1. The mixing layer was well outside the location of the jet flame of the inner burner, however, and had no observable influence on its flow and combustion properties (visualizations and measurements providing evidence of this behavior will be discussed later).

Hydrogen (99.95% purity) was supplied from commercial cylinders while dry air (dew point less than 240 K) was obtained from laboratory supplies. All gas flow rates were measured with rotameters, yielding a maximum uncertainty of fuel-equivalence ratios less than 12% at $\phi = 0.3$ with the proportionately lower values at higher fuel-equivalence ratios. The gases were mixed in a manifold and then flowed through long lines (length-to-diameter ratios of ca. 400) to achieve uniform mixtures at the burner inlets. In order to control flash-back, which was problematical due to the high flame speeds of hydrogen/air mixtures, flame arrestor screens were installed in the reactant lines of both burners at a location of 50 diameters upstream of the burner exit.

Fan-stirred bomb The fan-stirred bomb is described by Groff (1987). It is similar to

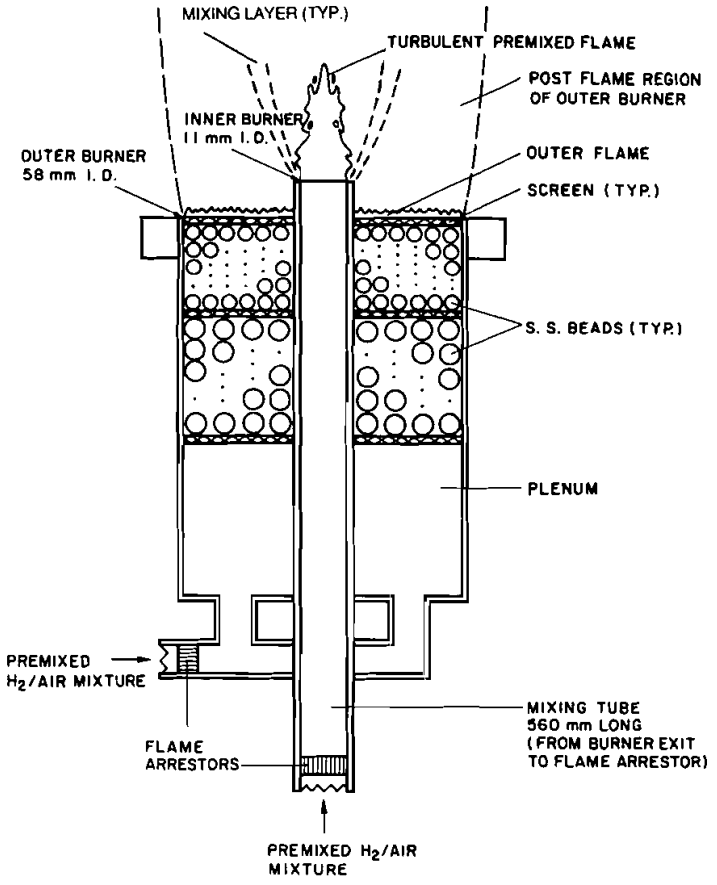

FIGURE 1 Sketch of the jet burner.

the arrangement used earlier by Semenov (1965) and Bradley and coworkers (Abdel-Gayed *et al.*, 1976, 1984; Andrews and Bradley, 1973). The chamber is quasi-spherical with a volume of 10 600 cc and a 260 mm crossectional diameter at the center. Optical access is provided by two 92 mm diameter quartz windows mounted opposite one another. Turbulence was generated by four fans (8 bladed, blade diameter of 135 mm, pitch of 45°) located at 90° intervals around the periphery of the vessel. The fans directed their flow toward the center of the vessel and operated at rotational speeds up to 2400 rpm.

The hydrogen and air sources were the same as the jet flame experiments. The proper partial pressures of hydrogen and air were mixed together using the fans and the flame was spark ignited at the center of the vessel using electrodes extending from the top and bottom. The spark gap was roughly 3 mm while the sparks had a duration of 0.5 ms and stored energies of 0.3 mJ.

Fansler (1989) measured the properties of the turbulent field produced by the fans using laser velocimetry. The turbulence is nearly isotropic over a region having a diameter of 80 mm at the center of the vessel. Mean velocities are negligible while velocity fluctuations vary linearly with fan speed over the present test range (0.44 m/s

at 600 rpm and 1.84 m/s at 2400 rpm)—relatively independent of pressure. Hot-wire measurements during the present investigation confirmed these results at atmospheric pressure—within experimental uncertainties.

Flow visualization Flash-Schlieren photographs and cinematography were used to visualize the jet and bomb flames, respectively. Both arrangements used 102 mm diameter parabolic reflectors, having focal lengths of 1220 mm, to collimate the light beam and focus it on the knife edge. The light source for the jet flames was a Xenon Corp., Model 457, Pulsar Flashlamp, yielding 10 J per pulse with a 1 μs flash duration. The flash duration was short enough to stop the flame and flame luminousity was not a problem; therefore, single photographs were taken in a darkened room using an open-camera shutter with Type 52 Polaroid film (100 × 125 mm, fine-grained ASA 400).

The light source for the fan-stirred bomb was an EG&G Model 3CP4 flash lamp with a PS-450 power supply having with a light intensity of 1 mJ/flash and a flash duration of 1 μs. The lamp was synchronized with the motion-picture camera. The flash-Schlieren photographs were recorded with a 16 mm high-speed camera operating at roughly 1000 pictures per second, using Tri-X negative film.

Rayleigh scattering The arrangement for the Rayleigh scattering measurements was similar to Gulati and Driscoll (1986). For hydrogen/air flames, Rayleigh-scattered light is a unique function of reactedness, within an accuracy of 3.7%. To measure the Rayleigh scattered light, the blue line of an argon-ion laser (488 nm with 2W of optical power) was focussed with a 80 mm focal length lens. The scattered light was collected at 90° from the laser beam using an f1.2 camera lens having a focal length of 85 mm. The collected light was then focussed on a photomultiplier tube (RCA 4526) through a laser-line filter (1.0 nm optical bandpass at 488 nm). The optical configuration yielded a measuring volume having a diameter of 250 μm and a length of 500 μm.

The output of the photomultiplier was amplified and low-pass filtered before digitization using a 14 bit A/D converter. The resulting signal was sampled at 50 kHz and stored as samples of 4096 records on a minicomputer. Since the hydrogen/air flames are thin, temporal records approximated telegraph signals as the measuring volume crossed between burned and unburned gas. At each location, the background signal and flame radiation were measured and found to contribute 6% to the Rayleigh signal and were subtracted. Shot noise also was determined at each location using a previously-measured calibration curve that related shot noise to the mean signal level. The shot noise contribution to the r.m.s. signal fluctuations was typically 8% and was subtracted; it does not contribute to the mean signal level. Several sets of records were processed to yield statistically-significant time-averaged mean and fluctuating reactiveness (defined as the fraction of time that burned gas was present). Uncertainties (95% confidence) of these measurements were dominated by gradient broadening and the finite number of samples that were processed: they are estimated to be less than 10%.

Laser velocimetry The arrangement of the laser velocimetry system was modified slightly from Gulati and Driscoll (1986). A dual-beam forward-scatter arrangement was used based on the green line of an argon-ion laser (514.5 nm with 2 W of optical power). The optical arrangement yielded a measuring volume having a diameter of 200 μm and a length of 870 μm. The region where measurements were made involved relatively-high velocities (10–120 m/s) and relatively-low turbulence intensities (less than 30%); therefore, it was not necessary to use frequency shifting to control directional bias and ambiguity.

TABLE I
Turbulent Jet Flame Test Conditions[a]

ϕ	$\bar{u}_{o,avg}$(m/s)[b]	$\bar{u}'_{o,avg}/S_L$[c]	L_c/d
Re = 7000, Re_t = 280:			
0.30	10.9	2.7	6.4
0.65	12.1 (13.4)	0.7	–
0.80	12.6	0.6	2.1
1.00	13.3	0.5	1.9
1.80	15.7	0.4	1.7
3.57	20.4	0.9	2.7
Re = 20000, Re_t = 800:			
0.00	27.9 (28.5)	–	–
0.30	31.0	7.8	7.5
0.80	36.0	1.6	3.7
1.00	37.9	1.4	3.2
1.80	45.0	1.3	3.3
3.57	58.3	2.5	7.7
Re = 40000, Re_t = 1800:			
0.30	62.1	15.5	8.5
0.65	69.1 (66.0)	3.7	–
0.80	72.0	3.3	5.4
1.00	75.8	2.8	4.8
1.80	90.0	2.6	5.3
3.57	116.4	5.0	11.7

[a] Concentric tube burner: inner tube, 11 mm inside diameter × 1 mm thick; outer tube, 58 mm inside diameter × 3 mm thick. Outer flame: ϕ = 0.3, Re = 3400, $\bar{u}_{o,avg}$ = 1 m/s. Hydrogen (99.95% purity)/air flames at atmospheric pressure.

[b] Based on measured flow rate. Numbers in parentheses denote LDA data averaged over burner exit.

[c] S_L from Andrews and Bradley (1973); $\bar{u}'_{o,avg}/\bar{u}_{o,avg}$ taken to be 10%.

The jet flow was seeded with aluminum oxide particles having a nominal diameter of 1 μm. The Doppler signals were processed with a burst counter and stored on a minicomputer. Mean and fluctuating velocities were then computed as ensemble averages, ignoring effects of velocity bias, since these effects were found to be small. Uncertainties (95% confidence) of these measurements were dominated by finite sampling times: they are estimated to be less than 7% for mean velocities and 14% for velocity fluctuations.

Test conditions

Turbulent jet flame test conditions are summarized in Table I. Measurements were completed for jet Reynolds numbers ($Re = \bar{u}_{o,avg}d/\nu_o$) of 7000, 20000 and 40000. These conditions correspond to turbulent Reynolds numbers ($Re_t = \bar{u}'_{o,avg}l/\nu_o$) of 280, 800 and 1800, where $l = 0.4d$ assuming fully-developed turbulent pipe flow at the burner exit (Laufer, 1954). Fuel-equivalence ratios were in the range 0.3–3.57 so that unstable ($\phi < 1.8$) and stable ($\phi > 1.8$) diffusive-thermal conditions were considered. Values of $\bar{u}'_{o,avg}/S_L$ were in the range 0.44–15.52, to vary the relative importance of laminar and turbulent flame propagation effects. Additionally, $\bar{u}'_{o,avg}/\bar{u}_{o,avg}$ at the burner exit was roughly 10%, so that $\bar{u}_{o,avg}/S_L$ varied in the range 4–155; this generally yielded conditions where mean flame angles with respect to the streamwise direction were small so that the boundary-layer approximations could be used to simplify predictions. Normalized flame lengths, L_c/d (based on the distance along the axis where $\tilde{c}_c = 0.5$) were in the range 1.7–11.7, and burner exit Richardson numbers were small (10^{-5}–10^{-3}); therefore, properties of the unburned gas were generally

dominated by burner exit conditions. In the following, ϕ and Re will be used to identify particular flame results. However, it should be recognized that other fundamental flame properties ($\bar{u}'_{o,avg}/S_L$, $\bar{u}_{o,avg}/S_L$, Re_t, etc.) vary when these parameters are changed, as summarized in Table I.

It was originally planned to operate the outer burner flame at the same fuel-equivalence ratio as the inner burner flame in order to provide an adiabatic combustion-gas environment for the inner flame that was being studied. However, this was found to be unnecessary. Present test conditions were well within the flammability limits for hydrogen/air flames; therefore, the properties of the outer flame had negligible influence on the structure of the inner flame, *e.g.*, the structure of the inner flame did not change even when the outer flame was turned off completely for present test conditions. This followed even for fuel-rich conditions, since eventual oxidation of the fuel rich combustion products of the inner flame occurred in a diffusion flame within the mixing layer that was well separated from the inner premixed flame (except at the point of flame attachment near the burner exit), *e.g.*, the diameter of the inner flame was in the range 0-d while the diameter of the mixing layer was in the range d–3d. Additionally, velocities within the unburned inner flame gases, that primarily control the structure of the inner flame, were little influenced by the ambient environment and generally preserved burner exit conditions for the present high Reynolds number inner burner flows (these results will be discussed later). Nevertheless, rather than operating the inner burner in an air environment, the outer burner was operated at $\phi = 0.3$ with an average burner exit velocity of 1 m/s for all test conditions. This preserved an adiabatic ambient environment for tests nearest flammability limits ($\phi = 0.3$), where the inner flame had largest diameters, and improved flow visualization and reduced entrainment rates to the inner flame, while controlling the costs of operating the outer burner over a lengthy test program.

Present test conditions are summarized on a flow regime map along the lines of Bray (1980) in Figure 2. Average jet exit conditions are used to define u' and l on the plots since the flames were dominated by unburned gas properties as noted earlier. Present tests are largely in the mixing-limited thin-flamelet regime ($\bar{u}' > S_L$,

Present test conditions are summarized on a flow regime map along the lines of Bray (1980) in Figure 2. Average jet exit conditions are used to define u' and l on the plots since the flames were dominated by unburned gas properties as noted earlier. Present tests are largely in the mixing-limited thin-flamelet regime ($\bar{u}' > S_L, \delta_L < l_K$). However, results at higher Reynolds numbers for $\phi = 0.3$ are in the mixing-limited thickened-flame regime ($\bar{u}' > S_L$, $\delta_L > l_K$) while measurements for $\phi \geqslant 0.8$ and $Re = 7000$ are in the wrinkled thin-flamelet regime due to relatively-low turbulence intensities and relatively-high laminar flame speeds at these conditions.

Measured time-averaged mean and fluctuating velocities near the burner exit are plotted as a function of radial distance in Figure 3. These measurements were made at $x/d = 0.18$, which was the position nearest the exit that could be completely traversed by the laser velocimetry system. Results are illustrated at all three Reynolds numbers for various values of ϕ, however, varying ϕ had little effect on the measurements. Measurements illustrated for $\phi = 0$ show that the flow was symmetric. Present mean velocity profiles are in good agreement with Nikuradse (1932) except near the edge of the flow where the developing mixing layer between the jet exit and the measuring location affects present measurements. Present measurements of turbulence intensities are somewhat higher than those of Laufer (1954), even in the region that is not affected by the mixing layer; however, these differences decrease as jet Reynolds numbers increase toward the value of 500 000 used by Laufer (1954). In general, the results illustrated in Figure 3 suggest that present burner exit conditions approximate fully-developed turbulent pipe flow at comparable Reynolds numbers.

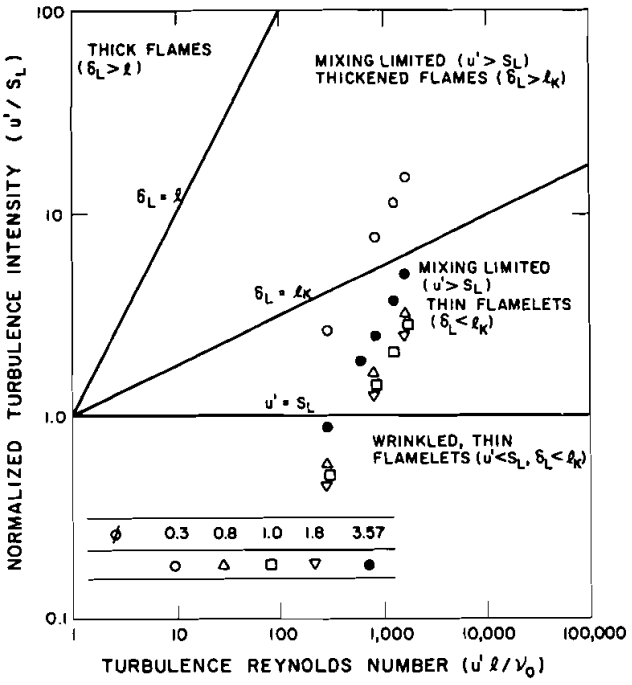

FIGURE 2 Turbulent flame regimes of the measurements.

THEORETICAL METHODS

General description

Flame length and statistical properties were predicted using a Favre-averaged turbulence model that is similar to that of Bray (1980) and Cant and Bray (1988), with some specific features from earlier work in this laboratory (Jeng and Faeth, 1984; Lee *et al.*, 1988). A major assumption was that the boundary-layer approximations apply. Even though the present flames were relatively short, this assumption is reasonable since the ratio of the radius of the burner to the location where the flames reached the axis (roughly $2L_c$) was generally less than 0.1. This implies that mean flame angles with respect to the streamwise direction were relatively small. Furthermore, measurements (to be discussed later) showed that increases of streamwise velocity fluctuations in the region of the flames, which is indicative of significant streamwise turbulent transport (Bray *et al.*, 1985), were only significant for the two shortest flames studied ($Re = 7000$ and $\phi = 1.0$ and 1.8, see Table I). Thus, streamwise turbulent transport, which often involves effects of counter-gradient diffusion, could be ignored while radial transport was treated using gradient-diffusion approximations based on earlier calibrations for constant- and variable-density turbulent round jets (Jeng and Faeth, 1984).

Other major assumptions of the formulation are as follows: (1) steady (in the mean) axisymmetric flow with no swirl; (2) low Mach number flow with negligible potential and kinetic energy changes, and negligible viscous dissipation in the mean; (3) negligible effects of radiant energy exchange; (4) equal exchange coefficients of all

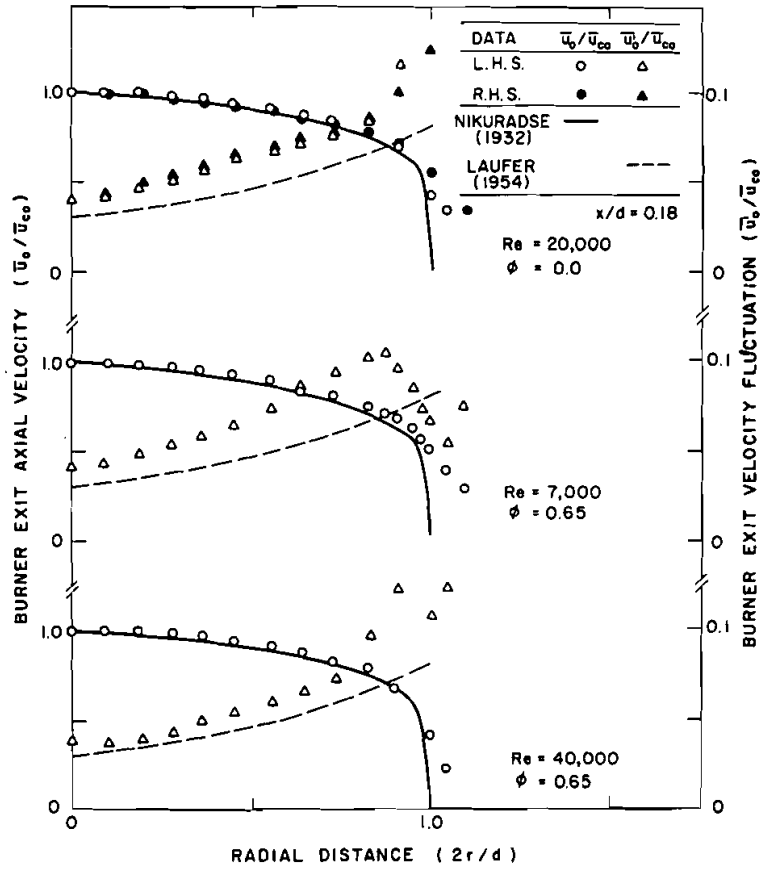

FIGURE 3 Streamwise mean and r.m.s. fluctuating velocities at the burner exit.

species and heat; (5) high Reynolds numbers so that laminar transport is negligible in comparison to turbulent transport; (6) negligible direct effects of buoyancy on turbulence properties; and (7) instantaneous separation of the flow field into regions of burned and unburned gas by an infinitely-thin flame. These assumptions are either representative of the conditions of the experiments or are typical of current turbulence models of premixed flames. For example, high burner exit velocities and short flame lengths imply small radiation numbers and thus negligible effects of radiant energy exchange. The assumption of equal exchange coefficients is widely used for turbulent flow while laminar transport, which would not satisfy this approximation due to the large mass diffusivity of the hydrogen, is not very important (aside from transport within the laminar flamelets that is not associated with bulk mixing) for Reynolds numbers on the order of 10^4. Furthermore, burner exit Richardson numbers are small (10^{-5}–10^{-3}) and the flames are short; therefore, direct effects of buoyancy on turbulence properties are small. Finally, present test conditions are generally within the thin-flamelet regime as discussed in connection with Figure 2.

Formulation

Under these assumptions, Bray (1980) shows that flow properties can be found by solving governing equations for conservation of mass, momentum, and reaction

TABLE II
Source Terms in the Governing Equations

G	S_G
1	0
$\tilde{u}$	$a(\rho_\infty - \tilde{\rho})$
$\tilde{c}$	$C_r\tilde{\rho}I_0S_L(1+\tau)\tilde{c}(1-\tilde{c})\varepsilon/((1+\tau\tilde{c})k^{3/2})$
k	$\mu_t(\partial\tilde{u}/\partial r)^2 - \tilde{\rho}\varepsilon$
ε	$(C_{\varepsilon 1}\mu_t(\partial\tilde{u}/\partial r)^2 - C_{\varepsilon 2}\tilde{\rho}\varepsilon)\varepsilon/k$

$C_r = g/(C_\mu^{3/4}|\sigma_y|)$

$$2I_0 = erfc\left(\frac{\ln(\varepsilon/\varepsilon_q) - \sigma^2/2}{2^{1/2}\sigma}\right) - \left(\frac{\varepsilon}{\varepsilon_q}\right) erfc\left(\frac{\ln(\varepsilon/\varepsilon_q) + \sigma^2/2}{2^{1/2}\sigma}\right)$$

C_μ	$C_{\varepsilon 1}$	$C_{\varepsilon 2}$	C_r	σ_c	σ_k	σ_ε	σ	$\lvert\sigma_y\rvert$	g
0.09	1.44	1.87	18.3	0.7	1.0	1.3	1.0	0.5	1.5

ϕ	0.3	0.8	1.0	1.8	3.57
$S_L(m/s)$[a]	0.4	2.2	2.7	3.5	2.3
$\varepsilon_q(m^2/s^3) \times 10^{-3}$[b]	0.47	262	504	1050	143

[a] From Andrews and Bradley (1973).
[b] $\varepsilon_q = \nu(S_L/\delta_L)^2$, $\delta_L = \alpha/S_L$.

progress variable, in conjunction with second-order turbulence model equations for turbulence kinetic energy and its rate of dissipation. The governing equations then take the following general form (Bray, 1980; Jeng and Faeth, 1984; Lee *et al.*, 1988):

$$\frac{\partial}{\partial x}(\bar{\rho}\tilde{u}G) + \frac{1}{r}\frac{\partial}{\partial r}(r\bar{\rho}\tilde{v}G) = \frac{1}{r}\frac{\partial}{\partial r}\left(r\frac{\mu_t}{\sigma_G}\frac{\partial G}{\partial r}\right) + S_G, \tag{1}$$

where $G = 1$ (for conservation of mass), $\tilde{u}$, $\tilde{c}$, k and ε. The turbulent viscosity was found as usual:

$$\mu_t = C_\mu\bar{\rho}k^2/\varepsilon. \tag{2}$$

The boundary conditions for Eq. (1) involve symmetry at the axis and a constant-property ambient environment, *e.g.*:

$$r = 0, \frac{\partial G}{\partial r} = 0; \qquad r \longrightarrow \infty, G = 0 (G \neq \tilde{c}), \tilde{c} = 1. \tag{3}$$

Since test results showed that the inner premixed flame considered during these computations was not affected by the properties of the outer burner flame, ambient gas properties of the inner flame were taken to be its combustion products. Initial conditions were defined at the burner exit where the flow was assumed to be fully-developed turbulent pipe flow; therefore, distributions of $\tilde{u}$, k and ε were obtained from Nikuradse (1932) and Laufer (1954), noting that time- and Favre-averaged quantities are identical for constant density flows and $\tilde{c} = 0$ by definition at the burner exit. The sensitivity of the predictions to variations of initial conditions, and to other parameters of the formulation, was examined and will be taken up later.

The source terms appearing in Eq. (1), S_G, are summarized in Table II, along with

all empirical constants. Except for $S_{\tilde{c}}$, all source terms and empirical constants are identical to earlier computations for axisymmetric turbulent flows in this laboratory (Jeng and Faeth, 1984; Lee *et al.*, 1988). These empirical constants were selected to match predictions and measurements for various constant- and variable-density noncombusting single-phase round jets and have yielded good predictions of the structure of turbulent jet diffusion flames (Jeng and Faeth, 1984); however, these values are not very different from early proposals of $k - \varepsilon$ turbulence models (Lockwood and Naguib, 1975).

Turbulent reaction was treated in two ways: (1) the mixing-limited approach used by Lee *et al.* (1988); and (2) the recent approach of Cant and Bray (1988) which provides for effects of flame stretch. The mixing-limited approach is based on Bray (1980) for thin-laminar flamelets where it is implied that the laminar flame speed is small in comparison to velocity fluctuations. This yields the following source term for $\tilde{c}$:

$$S_{\tilde{c}} = C_r \tilde{\rho} \tilde{c}(1 - \tilde{c})\varepsilon/k, \tag{4}$$

where $C_r = 1.87$ from Lee *et al.* (1988).

The approach of Cant and Bray (1988) is far more complex and is summarized in Table II. Values of the laminar flame speed are needed: they were obtained from Andrews and Bradley (1973) and are listed in Table II. Other parameters are discussed by Cant and Bray (1988): σ, $|\sigma_y|$, g and ε_q were based on their suggestions while matching predictions and measurements at $\phi = 3.57$ and $Re = 40\,000$. Matching other conditions was not possible without adopting values of σ, $|\sigma_y|$, and ε_q that were either beyond the ranges recommended by Cant and Bray (1988) or were not consistent with the measured laminar flame properties of Andrews and Bradley (1973).

Under the thin-flame approximation the flow only has instantaneous burned and unburned gas states. The unburned state is an initial condition; the burned state was found by assuming thermodynamic equilibrium for adiabatic constant-pressure combustion at atmospheric pressure using the Gordon and McBride (1971) code. Under the thin-flame approximation, c has a double-delta probability-density function and all mean and fluctuating scalar properties (including $\bar{c}$) are only functions of their values in the burned and unburned gas and $\tilde{c}$, see Bray (1980) or Lee *et al.* (1988) for specific formulas.

Calculations

The calculations employed the GENMIX algorithm of Spalding (1978). Present results involved 30 radial grid nodes with streamwise step sizes limited to less than 3% of the current flow width or a 5% increase of the mass flow rate of the jet—whichever was smaller. Doubling the number of grid nodes changed predictions less than 1%; therefore, numerical accuracy generally exceeds expected uncertainties of other aspects of the predictions.

The sensitivity of the predictions to variations of parameters in the formulation was also studied. The most sensitive parameters were k_0, ε_0 and C_r, where 50% increases of these quantities caused -20, 20 and -7% variations in predicted values of L_c. Since k_0 and ε_0 are known reasonably well for fully developed turbulent pipe flow, while C_r was selected to match one set of measurements, these results suggest that the predictions are relatively insensitive to parameters in comparison to the limitations of turbulence modeling itself.

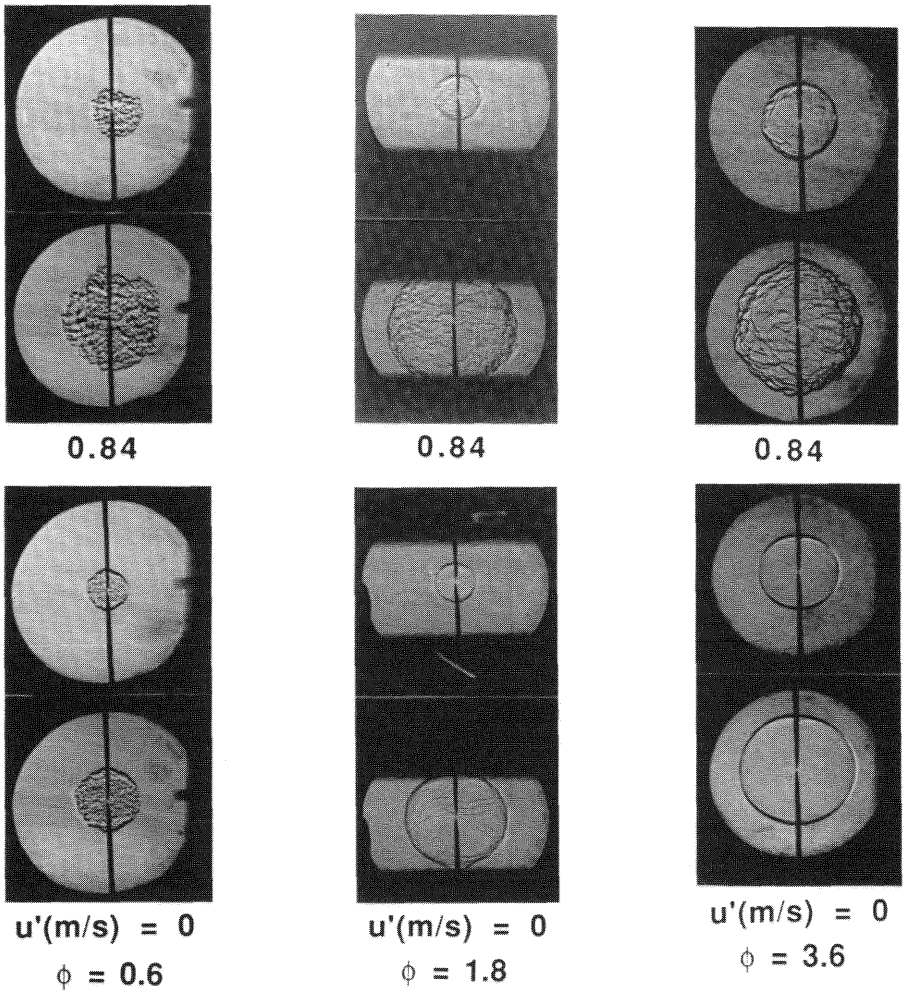

FIGURE 4 Flash-Schlieren photographs of the flames within the fan-stirred bomb. Note: $\phi = 0.6$, 1.8 and 3.6 correspond to unstable, neutral, and stable preferential-diffusion conditions, respectively.

RESULTS AND DISCUSSION

Flow Visualization

Flash-Schlieren photographs of combustion within the fan-stirred bomb provide a useful indication of diffusive-thermal effects since both quiescent and turbulent conditions could be observed. Some representative results are illustrated in Figure 4. Photographs of the flame at two instants after ignition are illustrated for unstable ($\phi = 0.6$), neutral ($\phi = 1.8$) and stable ($\phi = 3.6$) conditions at both quiescent and turbulent ($\bar{u}' = 0.84$ m/s) conditions. At quiescent conditions, the flame surface is relatively smooth for neutral and stable conditions but becomes spontaneously wrinkled shortly after ignition for unstable conditions. When the reactants are turbulent, the turbulence causes a wrinkled flame surface for all conditions; the presence of

turbulence significantly increases the degree of distortion of the flame surface even for unstable conditions. However, diffusive-thermal effects, analogous to those found by Clavin and coworkers (Clavin, 1985), can be seen by comparing the photographs for neutral and stable conditions. Neutral conditions presumably reflect the behavior of passive distortion of the flame surface by turbulence since diffusive-thermal effects are absent and effects of flame stretch are small due to modest turbulence levels and the high laminar flame speed. Thus, comparing this baseline result with the photographs for stable conditions suggests that diffusive-thermal effects have acted to reduce the distortion of the flame surface by turbulence for stable conditions. The results were similar for other test conditions: diffusive-thermal effects generally reduced flame distortion by turbulence for stable conditions ($\phi > 1.8$) and enhanced distortion for unstable conditions ($\phi < 1.8$), although the degree of enhancement was generally less apparent.

It was also possible to identify similar diffusive-thermal effects from the flash-Schlieren photographs of the turbulent jet flames. Some representative results for $\phi = 1.0$, 1.8 and 3.57 and $Re = 7000$, 20 000 and 40 000 are illustrated in Figure 5. Taking $\phi = 1.8$ as the neutral condition, where diffusive-thermal effects are minimized, it is clear that the flame surface for stable conditions ($\phi = 3.57$) is wrinkled to a lesser degree at comparable Reynolds numbers. In contrast, the flame surfaces for unstable conditions ($\phi = 1.0$) are somewhat more irregular (spiked), and have a greater number of detached islands of unreacted gas, than is observed for neutral conditions at the same Reynolds number. Thus, diffusive-thermal effects appear to be important for all fuel-equivalence ratios (except possibly near the neutral condition) even at relatively high Reynolds numbers.

The photographs of Figure 5 also show that the flame lengths increase dramatically as Re increases and are shortest near $\phi = 1.8$ where the laminar flame speed is a maximum (this is most evident for $Re = 7000$). This behavior will be discussed subsequently, based on the more quantitative measurements of reaction progress variable. Nevertheless, predictions based on the mixing-controlled turbulent reaction expression (Eq. (4)) could not reproduce these trends, yielding flame lengths, L_c, of ca. 10 for all test conditions. Therefore, only the Cant and Bray (1988) approach will be considered in the following in order to reduce cluttering of the plots with obviously ineffective predictions.

Finally, the Schlieren photographs of Fig. 5 help quantify the location of the mixing layer between the inner and outer burner flames for present test conditions. The layer can be seen most clearly for $Re = 7000$ and 20 000, where it appears as a dark-shaded area emanating from the left-hand side of the burner exit (a corresponding but less distinct light-shaded area appears at the right side of the photographs). As noted earlier, the primary jet burner flames are well inside the location of the mixing layer.

Unreactedness

Mean and fluctuating values of the reaction progress variable are simply related, since this variable yields a telegraph signal for the thin-flamelet conditions of present tests; this implies that $\bar{c}'^2 = \bar{c}(1 - \bar{c})$. This relationship was satisfied by measurements over the present test range within 15%; therefore, the following discussion will be limited to $\bar{c}$. Measured and predicted time-averaged unreactedness along the axis of the jet flames, $(1 - \bar{c})_c$, are illustrated in Figure 6 for $Re = 7000$, 20 000 and 40 000 at unstable ($\phi = 0.3$, 0.8, 1.0), neutral ($\phi = 1.8$) and stable ($\phi = 3.56$) conditions with respect to diffusive-thermal effects. Predictions are based on the Cant and Bray (1988)

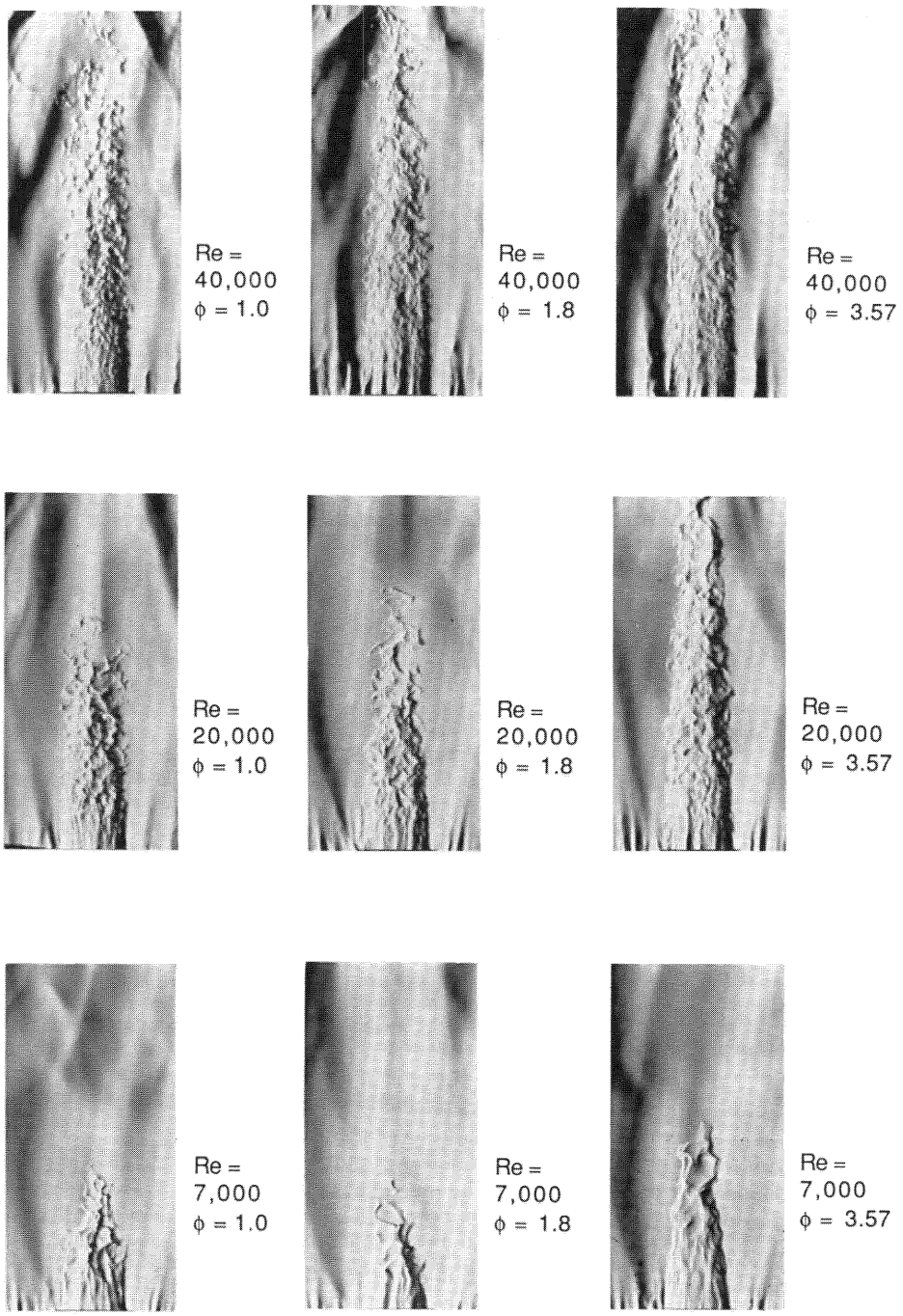

FIGURE 5 Flash-Schlieren photographs of jet flames. Note: ϕ = 1.0, 1.8 and 3.57 correspond to unstable, neutral, and stable preferential-diffusion conditions, respectively.

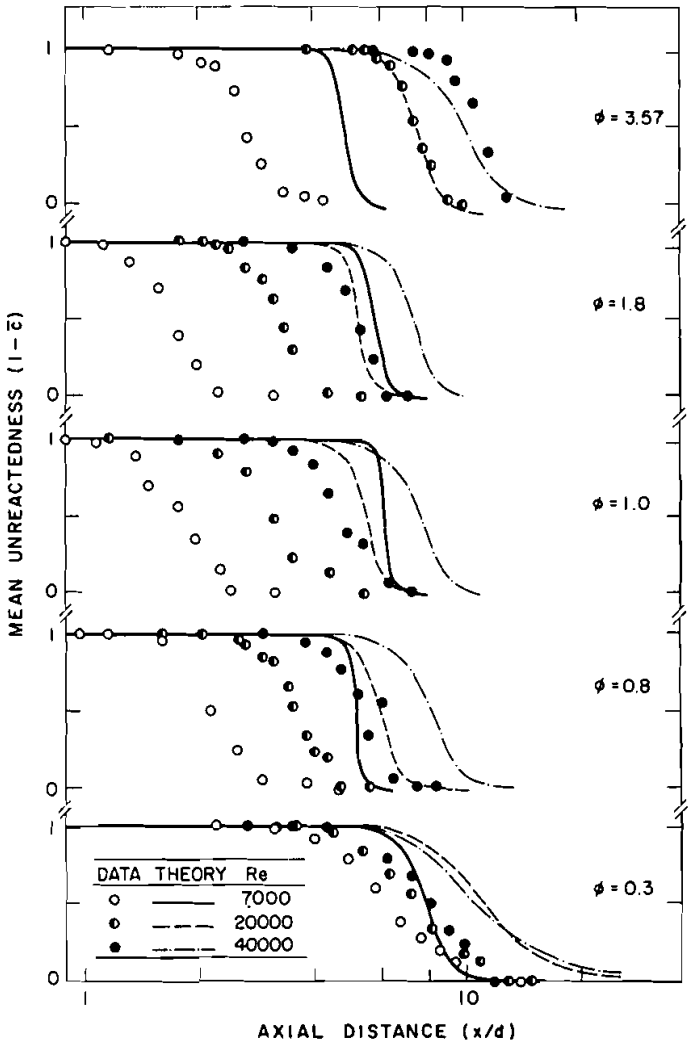

FIGURE 6 Mean unreactedness along the burner axis.

turbulent reaction model with parameters selected to match predictions and measurements at $\phi = 3.57$ and $Re = 40\,000$, as noted earlier.

A significant trend of the results illustrated in Figure 6 is that flame lengths increase with increasing Re for all values of ϕ. The increase is greatest for $\phi = 1.8$ where the laminar flame speed is relatively large in comparison to levels of turbulent fluctuations, *e.g.*, $\bar{u}'_{o,avg}/S_L$ is in the range of 0.4–2.6 at this value of ϕ which places most of these results in or near the wrinkled thin-flamelet regime ($\bar{u} < S_L$) illustrated in Figure 2. At these conditions, the turbulent burning velocity is dominated by laminar effects and only increases slightly due to increased turbulent velocity fluctuations (since $\bar{u}'/S_L$ is relatively small) as $\bar{u}_{o,avg}$ (and thus Re) increases, even though $\bar{u}'_{o,avg}/\bar{u}_{o,avg}$ is nearly constant for present test conditions. As a result, the flame stabilizes at a shallower angle with respect to the streamwise direction as $\bar{u}_{o,avg}$ (and thus Re)

increases and the flame length increases accordingly. Similarly, Re has the smallest effect on flame length at $\phi = 0.3$ where the laminar flame speed is relatively small in comparison to levels of turbulent fluctuations, *e.g.*, $\bar{u}'_{o,avg}/S_L \geq 6.4$ at this value of ϕ which places these results well into the mixing-limited thin-flamelet regime ($\bar{u}' > S_L$) illustrated in Figure 2. At these conditions, the turbulent burning velocity is dominated by turbulent effects and increases nearly proportional to increased turbulent velocity fluctuations as $\bar{u}_{o,avg}$ (and thus Re) increases, since $\bar{u}'_{o,avg}/\bar{u}_{o,avg}$ is nearly constant. In this case, the increased turbulent burning velocity nearly compensates for the increased burner exit velocity so that the flame position is nearly independent of $\bar{u}_{o,avg}$ (and thus Re). By definition, the flame length should be nearly independent of Re as mixing-limited conditions are approached. Thus, in view of the behavior seen in Figure 6, the order-of-magnitude estimate of the boundary between the wrinkled and the mixing-limited thin-flamelet regimes illustrated in Figure 2 would be improved by locating it at $\bar{u}' \approx 3S_L$.

In addition to direct effects of laminar flame speeds, the results illustrated in Figure 6 also exhibit effects of diffusive-thermal phenomena. For example, the flame length for $\phi = 3.57$ and $Re = 40\,000$ is longer than the rest, even the results approaching the mixing-controlled limit at $\phi = 0.3$ where the laminar flame speed is much lower. This suggests that diffusive-thermal phenomena at the stable condition are acting to reduce the distortion of the flame surface so that the required area to complete reaction can only be achieved by an increased flame length. Certainly quenching effects do not offer an explanation for this trend since the laminar flame speed for $\phi = 3.57$ is nearly an order-of-magnitude greater than $\phi = 0.3$, which should reverse the trend seen in Figure 6. Similarly, flame lengths for $\phi = 0.8$ and 1.0 are shorter than the neutral condition, $\phi = 1.8$, even though their laminar flame speeds are smaller: this suggests that diffusive-thermal phenomena at unstable conditions are acting to increase wrinkling of the flame surface so that the required area to complete reaction can be achieved in a shorter flame length. Naturally, $\bar{u}'_{o,avg}/S_L$ also plays a role in the required flame length, as discussed earlier; present results will be viewed directly in these terms later.

The combined effects of $\bar{u}'_{o,avg}/S_L$ varying in the range 0.4–15.5 and diffusive-thermal phenomena, for the present measurements, are not explicitly considered in the Cant and Bray (1988) combustion model. Thus, it is not surprising that there is only fair agreement between measurements and predictions illustrated in Figure 6. The main deficiency of the predictions is that the effect of Reynolds number is underestimated. Furthermore, since diffusive-thermal effects are not considered in the model, fitting the results at a stable condition ($\phi = 3.57$) causes predictions for neutral and unstable conditions to overestimate flame lengths. Finally, predictions are rather sensitive to the fit of the quenching correction: this causes flame lengths to reach a minimum at intermediate Re for some conditions (see $\phi = 1.0$ and 1.8) which is not observed experimentally. It appears that substantial extension of models of turbulent reaction in premixed flames will be required to treat many of the trends observed for hydrogen/air flames.

The measured and predicted radial variation of unreactedness are illustrated in Figure 7 for $\phi = 0.8$, 1.8 and 3.57 and $Re = 40\,000$. Results for other test conditions, however, were similar. The coordinates are highly normalized; therefore, the measurements exhibit a crude similarity at each x/L_c. This follows from the roughly triangular shape of the mean flame position in a plane through its axis, which is somewhat reflected by the flash-Schlieren photographs of Figure 4, *i.e.*, all flames have the same base dimension and thus roughly the same width at equal fractions of their height. The predictions are in fair agreement with the measurements at $x/L_c = 0.25$ and 1.0;

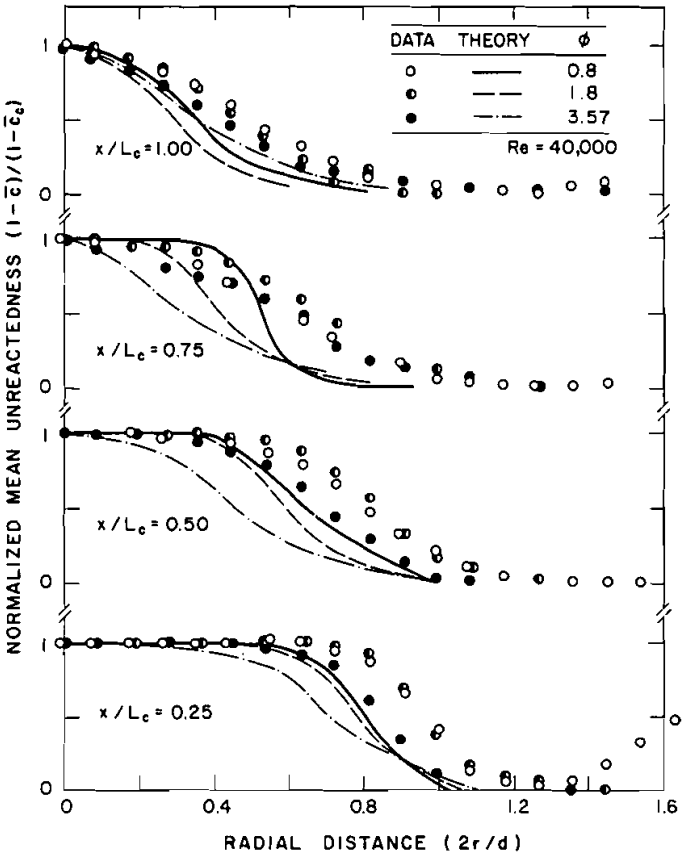

FIGURE 7 Radial profiles of mean unreactedness.

however, this is largely an artifact of the normalization of the results (centerline values of $\tilde{c}$ are not predicted very well) and the nearness of these locations to prescribed boundary conditions at the burner exit and the flame tip. In contrast, predictions at intermediate locations are not in good quantitative agreement with the measurements and exhibit variations with ϕ that are not observed.

Turbulent Burning Velocities

In an effort to quantify diffusive-thermal effects on the properties of the turbulent flames, effective turbulent burning velocities were computed. This involved defining an effective conical flame surface having a base diameter equal to the burner exit diameter and a height equal to L_c. The effective turbulent burning velocity, $S_{T,\text{eff}}$, was then defined as the mean velocity normal to this surface, assuming that the mean streamwise velocity was the same as at the burner exit. This assumption is justified because all flames for which $S_{T,\text{eff}}$ was computed lie within the potential core of the jet, where the velocity does not vary in the axial direction, as shown later. This method of using the mean flame location to define an effective angle between the turbulent flame and the incoming reactant velocity has been commonly used to determine

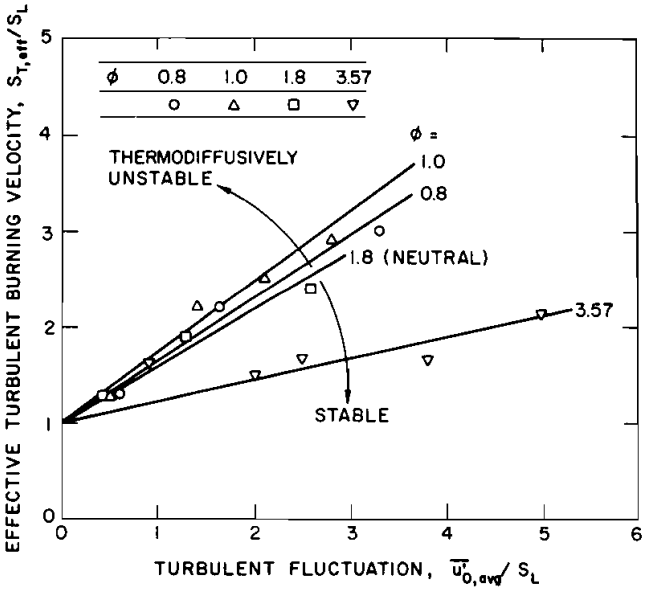

FIGURE 8 Effective turbulent burning velocity as a function of velocity fluctuations.

turbulent burning velocity (Ballal, 1979; Grover *et al.*, 1959; Wohl *et al.*, 1953; Cheng and Ng, 1984; Dandekar and Gouldin, 1982; Driscoll and Gulati, 1988).

The resulting effective turbulent burning velocities are illustrated in Figure 8, which is a plot of $S_{T,\text{eff}}/S_L$ as a function of $\bar{u}'_{o,avg}/S_L$. The values of S_L used for these correlations were obtained from Andrews and Bradley (1973) and are summarized in Table II. Results plotted in Figure 8 include $\phi = 0.8$, 1.0, 1.8 and 3.57 for *Re* in the range 7000–40 000. The measurements illustrated indicate that effective turbulent flame speeds fall on two branches: a neutral-unstable branch involving $\phi = 0.8$, 1.0 and 1.8, and a stable branch involving $\phi = 3.57$. The stable branch has substantially less response to increased turbulence levels (*i.e.*, smaller slope) than the neutral-unstable branch. Furthermore, even within the neutral-unstable branch, unstable conditions are somewhat more responsive to increased turbulence levels than the neutral condition. These trends clearly imply that diffusive-thermal phenomena retard turbulent distortion of the flame surface for stable conditions (thus yielding lower values of $S_{T,\text{eff}}$), and, to a lesser degree, enhance distortion for unstable conditions (yielding higher values of $S_{T,\text{eff}}$).

Other measurements in the literature yield similar behavior. For example, Abdel-Gayed *et al.* (1976, 1984) measured turbulent burning velocities of hydrogen/air mixtures at various ϕ using a fan-stirred bomb. When these measurements are correlated in the same manner as Figure 8, two branches are also observed: results for $\phi = 0.42$–1.58 yielding an unstable branch, and results for $\phi = 3.57$ yielding a stable branch having a smaller response to increased turbulence levels. Abdel-Gayed *et al.* (1976) attribute the reduced response for $\phi = 3.57$ to quenching, however, since S_L for this condition actually exceeds values for some of the conditions in the unstable branch, diffusive-thermal phenomena must play an important role in this behavior. Liu and Lenze (1988) measured turbulent burning velocities of CH_4-H_2/air mixtures stabilized at a stagnation point. They also find that rich flames have reduced response

to increased turbulence levels in comparison to lean flames but do not propose a reason for this behavior. Based on present results, this effect probably involves diffusive-thermal phenomena.

Taken together, these results suggest that diffusive-thermal phenomena influence the rate of propagation of turbulent flames at all but neutral conditions for high Reynolds numbers as well as low Reynolds numbers. Stable conditions tend to reduce distortion of the flame surface by the turbulence and, to a lesser degree, unstable conditions tend to enhance distortion of the flame surface by turbulence. These effects may explain past difficulties in obtaining correlations of turbulent flame speeds along the lines of Figure 8, as well as reliable models of turbulent combustion for premixed flames. Finding a rational way to incorporate diffusive-thermal effects into methods of estimating turbulent flame speeds has important implications, *e.g.*, most practical premixed turbulent flames, like those of spark ignition automotive engines, involve reactant systems having widely varying mass diffusivities and operate at stable conditions where diffusive-thermal effects are likely to significantly retard distortion of the flame surface by turbulence.

Velocities

Measured and predicted mean and r.m.s. fluctuating streamwise velocities along the axis of the jet flames are illustrated in Figures 9 and 10. Results are illustrated for $\phi = 0.3$, 1.0, 1.8 and 3.57 at $Re = 7000$ and 40 000. Measured characteristic flame lengths, L_c, with their uncertainties denoted by brackets, are also marked on the plots. Except for some jumps in the region of the flame for $Re = 7000$, which will be taken up later, the measurements in Figures 9 and 10 indicate little change from burner exit velocities until $x/d > 10$. This is a rather extended potential core for fully developed turbulent pipe flow at the burner exit, *e.g.*, Chuech *et al.* (1989) find potential core lengths of ca. $x/d = 4$ for constant-density gas jets with fully-developed pipe flow at the jet exit. The reason for this behavior is that the flow of reactants along the axis is surrounded by hot combustion products from its own flame as well as the hot gas flow from the outer burner. Thus, the low density of the surroundings reduces the entrainment rates of the jet which extends the length of the potential core.

Except for $\phi = 1.8$, 1.0 and 3.57 (to a lesser degree) at $Re = 7000$, mean and r.m.s. fluctuating velocities in Figures 9 and 10 are not particularly influenced by the presence of the flames. This behavior can be explained by changes in the average angle of the flames with respect to the mean flow direction, along the lines of Bray *et al.* (1985). The conditions where streamwise velocities, particularly streamwise r.m.s. velocity fluctuations, increase in the vicinity of the flame, all involve the shortest flames that have the largest average angles with respect to the flame axis. Then, velocity increases normal to the flames, due to the density ratio of the flames, have the largest component in the streamwise direction, yielding the highest streamwise r.m.s. velocity fluctuations due to flame intermittency at the measuring location, similar to past velocity measurements for oblique flames (Gulati and Driscoll, 1986). Thus, the results illustrated in Figure 10 suggest that effects of streamwise transport are generally small, justifying the use of boundary-layer approximations for present predictions, with the possible exception of $Re = 7000$ and $\phi = 1.0$ and 1.8, as discussed earlier. Recognizing the extended length of the potential core, and the small changes of the streamwise velocity (particularly for high Reynolds numbers), use of burner exit conditions to characterize the turbulence properties of the unburned gas appears to be justified for present test conditions.

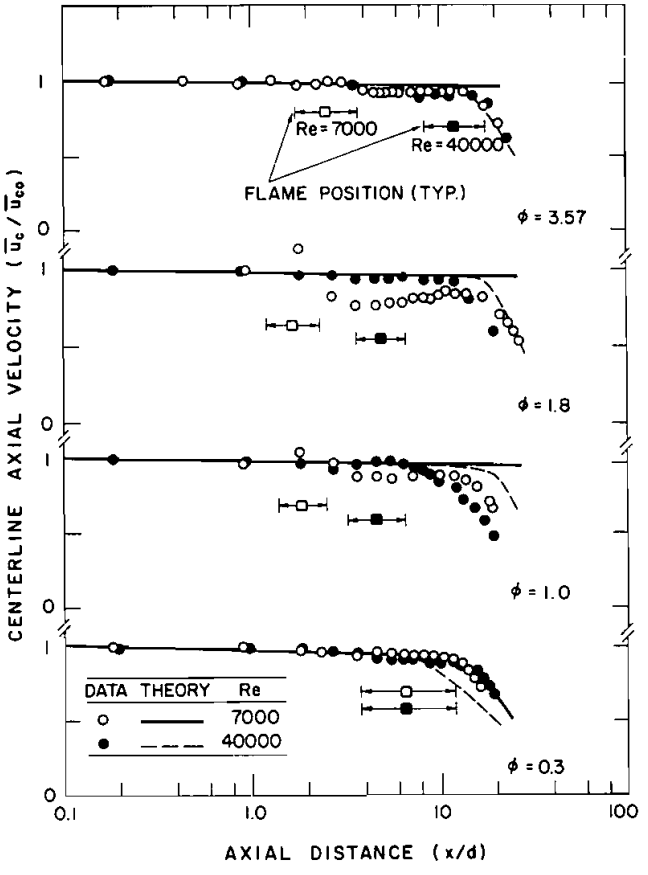

FIGURE 9 Streamwise mean velocities along the axis.

CONCLUSIONS

The major conclusions of the study can be summarized as follows:

1. In quiescent environments, hydrogen/air flames exhibit diffusive-thermal (preferential-diffusion) instabilities for fuel-equivalence ratios less than the maximum laminar flame velocity (ϕ = 1.8), as determined from Schlieren photographs.
2. Diffusive-thermal effects, similar to those described by Clavin (1985) for weakly-turbulent flames, persisted for the present high Reynolds number hydrogen/air turbulent jet flames. In particular, the turbulent distortion of the flame surface, and the response of profiles of unreactiveness and effective turbulent burning velocities to increased turbulence levels, were all damped for stable conditions; to a lesser degree, these properties were all enhanced for unstable conditions.
3. Diffusive-thermal damping effects at stable conditions are of particular importance: the effect was stronger than enhancement at unstable conditions for present test conditions; and many practical premixed flames involve high molecular weight fuels and operate lean, which places them in the diffusive-thermal stable regime. Thus, the tendency of some previous studies to assume that stable conditions are

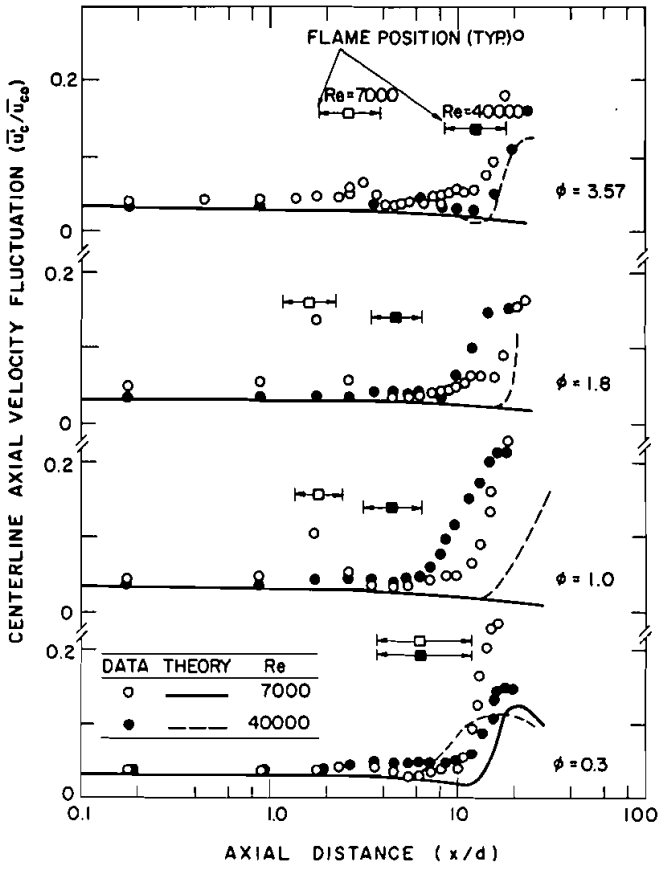

FIGURE 10 Streamwise r.m.s. velocity fluctuations along the axis.

not affected by diffusive-thermal effects can be erroneous. Correlations, and notions of modeling turbulent premixed flames, should be reexamined to consider diffusive-thermal effects.

4. Estimates of flame properties based on a contemporary turbulence model due to Cant and Bray (1988), which allows for effects of flame stretch, yielded only fair agreement with measurements; extensions to improve estimates of the effect of burner exit Reynolds numbers (or $\bar{u}_{o,avg}$ and $\bar{u}'_{o,avg}/S_L$) and to allow for diffusive-thermal phenomena are needed to treat hydrogen/air turbulent jet flames—even at high Reynolds numbers within the mixing-limited thin-flamelet regime.
5. Mean and r.m.s. fluctuating streamwise velocities along the axis generally did not vary significantly within the flame brush at high Reynolds numbers since the flames were oriented at a relatively small angle with respect to the flame axis at these conditions.
6. Present flames were not influenced by shear layer generated turbulence because they were within the potential core; thus, the flames only saw a turbulent field dominated by flow properties at the jet exit (fully-developed pipe flow).

ACKNOWLEDGEMENTS

This research was supported by the Office of Naval Research, Contract No. N00014-87-K-0698, with S. Ramberg serving as Scientific Program Officer. The authors also wish to thank E. G. Groff for many useful discussions and General Motors Research Laboratories for the loan of the fan-stirred bomb.

REFERENCES

Abdel-Gayed, R.G. and Bradley, D. (1976). Dependence of turbulent burning velocity on turbulent Reynolds number and ratio of laminar burning velocity to r.m.s. turbulent velocity. *Sixteenth Symposium (International) on Combustion*, The Combustion Institute, Pittsburgh, pp. 1725–1735.

Abdel-Gayed R. G., Bradley, D., Hamid, M. N., and Lawes, M. (1984). Lewis number effects on turbulent burning velocity. *Twentieth Symposium (International) on Combustion*, The Combustion Institute, Pittsburgh, pp. 505–512.

Andrews, G. E. and Bradley, D. (1973). Determination of burning velocity by double ignition in a closed vessel. *Combust. Flame* **20,** 77.

Ballal, D. R. (1979). The structure of a premixed turbulent flame. *Proc. R. Soc. London A* **367,** 353.

Boyer, L., Clavin, P., and Sabathier, F. (1980). Dynamic behavior of a premixed turbulent flame front. *Eighteenth Symposium (Interational) on Combustion*, The Combustion Institute, Pittsburgh, pp. 1041–1409.

Bray, K.N.C. (1980). Turbulent flows with premixed reactants. In P. A. Libby and F. A. Williams (Eds.), *Turbulent Reacting Flows*, Springer, Berlin, pp. 115–183.

Bray, K. N. C., Libby, P. A., and Moss, J. B. (1985). Unified modeling approach for premixed turbulent combustion-part I: general formulation. *Combust. Flame* **61,** 87.

Cant, R. S. and Bray, K. N. C. (1988). Strained laminar flamelet calculations of premixed turbulent combustion in a closed vessel. *Twenty-Second Symposium (International) on Combustion*, The Combustion Institute, Pittsburgh, pp. 791–799.

Cheng, R. K. and Ng, T. T. (1984). On defining the turbulent burning velocity in premixed V-shaped turbulent flames. *Combust. Flame* **57,** 155.

Chuech, S. G., Lai, M.-C., and Faeth, G. M. (1989). Structure of turbulent sonic underexpanded free jets. *AIAA J.* **27,** 549.

Clavin, P. (1985) Dynamic behavior of premixed flame fronts in laminar and turbulent flows. *Prog. Energy Combust. Sci.* **11,** 1.

Clavin, P. and Williams, F. A. (1979). Theory of premixed-flame propagation in large-scale turbulence. *J. Fluid Mech.* **90,** 589.

Clavin, P. and Williams, F. A. (1982). Effects of molecular diffusion and of thermal expansion on the structure and dynamics of premixed flames in turbulent flows of large scale and low intensity. *J. Fluid Mech.* **116,** 251.

Dandekar, K. V. and Gouldin, F. C. (1982). Temperature and velocity measurements in premixed turbulent flames. *AIAA J.* **20,** 652.

Driscoll, J. F. and Gulati, A. (1988). Measurement of various terms in the turbulent kinetic energy balance within a flame and comparison with theory. *Combust. Flame* **72,** 131.

Fansler, T. D. (1989). Turbulence characteristics of a fan-stirred combustion vessel. *Combust. Flame*, in press.

Gordon, S. and McBride, B. J. (1971). Computer program for calculations of complex chemical equilibrium compositions, rocket performance, incident and reflected shocks, and Chapman-Jouguet detonations. NASA Report SP-273. Washington.

Groff, E. G. (1982). The cellular nature of confined spherical propane-air flames. *Combust. Flame* **48,** 51.

Groff, E. G. (1987). An experimental evaluation of an entrainment flame-propagation model. *Combust. Flame* **67,** 153.

Grover, J. H., Fales, E. and Scurlock, A. C. (1959). Turbulent flame studies in a two-dimensional open burner. *ARS J.* **26,** 275.

Gulati, A. and Driscoll, J. F. (1986). Velocity-density correlations and Favre averages measured in a premixed turbulent flame. *Combust. Sci. and Tech.* **48,** 285.

Halstead, M. P., Pye, D. B. and Quinn, C. P. (1974). Laminar burning velocities and weak flammability limits under engine-like conditions. *Combust. Flame* **22,** 89.

Jeng, S.-M. and Faeth, G. M. (1984). Species concentrations and turbulence properties in buoyant methane diffusion flames. *J. Heat Trans.* **106,** 721.

Jones, W. P. and Whitelaw, J. H. (1982). Calculation methods for reacting turbulent flows: a review. *Combust. Flame* **48,** 1.

Laufer, J. (1954). Cited in Hinze, J. O. (1975), *Turbulence*, McGraw-Hill, New York, 2nd edition, pp. 720–724.

Lee, T.-W., Gore, J. P., Faeth, G. M., and Birk, A. (1988). Analysis of combusting high-pressure monopropellant sprays. *Combust. Sci. and Tech.* **57,** 95.

Lewis, B. and von Elbe, G. (1961). *Combustion, Flames and Explosions of Gases*, 2nd edition, Academic Press, New York, pp. 381–384.

Libby, P. A., Sivasegaram, S., and Whitelaw, J. H. (1986). Premixed combustion. *Prog. Energy Combust. Sci.* **12,** 353.

Liu, Y. and Lenze, B. (1988) The influence of turbulence on the burning velocity of premixed CH_4-H_2 flames with different laminar burning velocities. *Twnety-Second Symposium (International) on Combustion*, The Combustion Institute, Pittsburgh, pp. 747–754.

Lockwood, F. C. and Naguib, A. S. (1975). The prediction of the fluctuations in the properties of free, round jet, turbulent diffusion flames. *Combust. Flame* **24,** 109.

Manton, J., von Elbe, G. and Lewis, B. (1952). Nonisotropic propagation of combustion waves in explosive gas mixtures and the development of cellular flames. *J. Chem. Phys.* **20,** 153.

Markstein, G. H. (1951). Experimental and theoretical studies of flame-front stability. *J. Aero. Sci.* **18,** 199.

Nikuradse, J. (1932). Cited in Hinze, J. O. (1975), *Turbulence*, McGraw-Hill, New York, 2nd edition, pp. 725–727.

Searby, G. and Clavin, P. (1986). Weakly turbulent, wrinkled flames in premixed gases. *Combust. Sci. and Tech.* **46,** 167.

Semenov, E. S. (1965). Measurement of turbulence characteristics in a closed volume with artificial turbulence. *Combustion, Explosion and Shock Waves* **1,** 57.

Spalding, D. B. (1978). *GENMIX: A General Computer Program for Two-Dimensional Parabolic Phenomena*. Pergamon Press, Oxford.

Williams, F. A. (1985). *Combustion Theory*, 2nd edition, Benjamin/Cummings, Menlo Park, CA, pp. 341–372, 411–445.

Wohl, K., Shore, L., Rosenberg, H., and Weil, J. H. (1953). Burning velocity of turbulent flames. *Fourth Symposium (International) on Combustion*, The Combustion Institute, Pittsburgh, pp. 620–644.